Long-term accumulation of carbonate shells reflects a 100-fold drop in loss rate

Adam Tomašových[1]*, Susan M. Kidwell[2], Rina Foygel Barber[3], and Darrell S. Kaufman[4]
[1]Geological Institute, Slovak Academy of Sciences, Dubravska cesta 9, 84005 Bratislava, Slovakia
[2]Department of Geophysical Sciences, University of Chicago, 5734 S. Ellis Avenue, Chicago, Illinois 60637, USA
[3]Department of Statistics, University of Chicago, 5734 S. University Avenue, Chicago, Illinois 60637, USA
[4]School of Earth Sciences and Environmental Sustainability, Northern Arizona University, Campus Box 4099, Flagstaff, Arizona 86011, USA

ABSTRACT

Shells in modern seabeds can be thousands of years old, far older than would be extrapolated from the rapid rates of shell loss detected in short-term experiments. An extensive shell-dating program on the Southern California (USA) shelf permits rigorous modeling of the dynamics of shell loss in the mixed layer, discriminating the key rates of carbonate disintegration and sequestration for the first time. We find that bivalve shells experience an initially high disintegration rate λ_1 (~ decadal half-lives) but shift abruptly, within the first ~500 yr postmortem, to a 100-fold lower disintegration rate λ_2 (~ millennial half-lives) at sequestration rate τ (burial and/or diagenetic stabilization). This drop permits accrual of a long tail of very old shells even when sequestration is very slow, and allows only a minority (<1%) of all shells to survive the first phase. These high rates of disintegration and low rates of sequestration are consistent with independent measures of high carbonate loss and slow sedimentation on this shelf. Our two-phase model thus reveals significant spatial and temporal partitioning of carbonate loss rates within the mixed layer, and shows how shell age-frequency distributions can yield rigorous and realistic estimates of carbonate recycling on geological time scales.

INTRODUCTION

Relictual sediments rich in carbonate shells are widespread on modern continental shelves (Emery, 1968). Radiocarbon dating, motivated both to constrain the timing of post-glacial sea-level rise and to estimate scales of time-averaging, reveals that shells can persist in the mixed layer of the seabed for millennia (Kidwell and Bosence, 1991; Flessa and Kowalewski, 1994; Kidwell et al., 2005; Edinger et al., 2007; Krause et al., 2010; Kosnik et al., 2009, 2013), notwithstanding short-duration experiments that find high rates of shell loss, with half-lives of a few months, years, or decades (Cummins et al., 1986; Powell et al., 2006, 2011). Fitting shell age-frequency distributions (AFDs) with a simple exponential model of constant shell loss analogous to radiometric decay does not resolve this paradox and commonly does not approximate AFD shapes (Olszewski, 1999). Mechanistically, this approach also cannot differentiate the two distinct modes of shell loss, namely disintegration and burial (Meldahl et al., 1997). Analytical models that can discriminate loss rates are thus needed to resolve the paradox of millennial-scale persistence of shell carbonate. Understanding the dynamics of shell loss is fundamental to the temporal resolution and completeness of paleobiological and geochemical data drawn from fossil assemblages, as well as to carbonate burial and buffering capacity, a growing concern with ocean acidification (Waldbusser et al., 2011).

Here, we present the results of a large-scale shell-dating effort of two aragonitic bivalve species on the Southern California (USA) continental shelf, and use a novel likelihood, model-selecting approach to assess the dynamics of shell loss. We find a discrete, two-phase dynamic, where the timing of a drop in disintegration rate is controlled by a sequestration rate that operates at millennial scales. Although the idea of sequestration as a means of reducing shell loss has emerged repeatedly from stratigraphic and actualistic inference (Aller ,1982; Kidwell, 1986; Morse and Casey, 1988; Kowalewski et al., 1998), time-lapse studies (Glover and Kidwell, 1993; Best et al., 2007; Powell et al., 2011), and simulations (Sadler, 1993; Olszewski, 2004), our study produces the first analytic estimates of disintegration and sequestration rate from AFD data.

METHODS

AFDs were quantified for two shallow-burrowing bivalves, *Nuculana taphria* (n = 232) and *Parvilucina tenuisculpta* (n = 234), both sampled in 2003 with 0.1 m^2 Van Veen grabs at 18 sites between 19 m and 72 m water depth on the Southern California continental shelf, where living populations of these two species also occur (Table DR1 in the GSA Data Repository[1]). Grabs penetrated the sediment to a depth of 7–15 cm; ^{210}Pb evidence indicates that the decadal-scale mixed layer is 10–15 cm thick (Alexander and Lee, 2009). Enantiomeric D/L ratios of aspartic acid and glutamic acid were established with amino acid racemization analysis. Eight specimens of *Parvilucina* and 11 specimens of *Nuculana* were dated by accelerator mass spectrometry ^{14}C to calibrate D/L values (Table DR2). ^{14}C ages were calibrated to calendar years using Calib6.0 (Stuiver and Reimer, 1993) and a regional marine reservoir correction ΔR of 234 yr (standard deviation = 96 yr). D/L values were raised to a power-law exponent *e* that minimized differences between the measured ^{14}C age and the age predicted by the linear relationship between D/L^e and the calibrated ^{14}C age. Eight AFDs were produced by pooling shells into regional-scale, single-species assemblages corresponding to four shelf segments between Santa Barbara and San Diego, California (Fig. DR1 in the Data Repository).

Loss rate is determined by processes that destroy the taxonomic identifiability of a shell (disintegration) or remove it from a mixed layer by burial (or transportation, which is assumed to be minor; Kidwell, 2013). We evaluated three probability density functions to estimate shell loss rates from AFDs that actively receive new dead shells. Each density function corresponds to a different model of how the instantaneous per-individual shell loss rate is partitioned within the mixed layer, specifically between a taphonomically active zone (TAZ) with high disintegration rates (Davies et al., 1989) and a sequestration zone (SZ) with low disintegration rates (Olszewski, 2004) (Fig. 1). These two zones can exist as discrete, surficial and deeper layers (Figs. 1B and 1C). Alternatively, the SZ can comprise patchy microenvironments within the TAZ that favor carbonate reprecipitation (cf. Aller, 2014), or formerly sequestered shells can be admixed with highly reactive shells back in the TAZ if shells undergo burial-exhumation cycles. Because individual shells are collected before their final loss from the mixed layer, their age underestimates their actual postmortem per-

*E-mail: geoltoma@savba.sk.
[1]GSA Data Repository item 2014295, details on methods, and raw data on shell ages, is available online at www.geosociety.org/pubs/ft2014.htm, or on request from editing@geosociety.org or Documents Secretary, GSA, P.O. Box 9140, Boulder, CO 80301, USA.

GEOLOGY, September 2014; v. 42; no. 9; p. 819–822; Data Repository item 2014295 | doi:10.1130/G35694.1 | Published online 29 July 2014

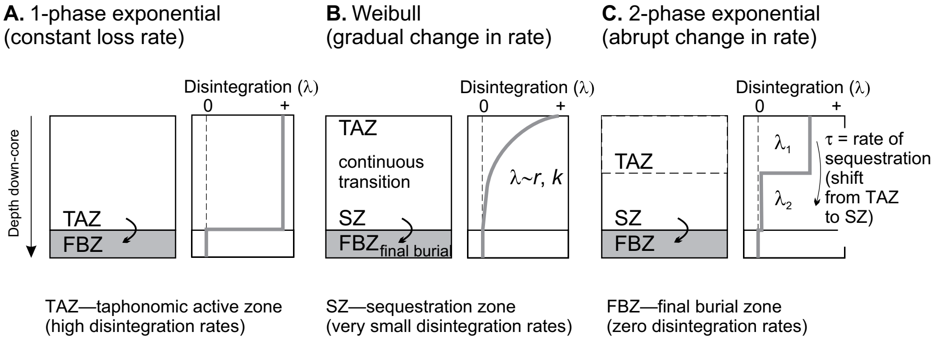

Figure 1. Conceptual partitioning of disintegration and burial. Death assemblages accumulate in the mixed layer (white layer in left column of each pair), where shells are subject to loss rate λ. λ is determined by the disintegration rates that a shell experiences in a taphonomically active zone (TAZ) and in a sequestration zone (SZ), by its sequestration rate τ to a SZ, and by its rate of final burial (FBZ, gray layer). A: λ is constant regardless of shell position within the mixed layer. B: λ declines gradually with depth as a function of the Weibull parameters *r* and *k*. C: λ declines abruptly from a TAZ with high disintegration rate λ_1 into a SZ with much lower disintegration rate λ_2. This shift is determined by the net sequestration (burial or stabilization) rate τ.

sistence in the mixed layer. Our density functions are thus right-censored (Gelman et al., 2004): we compute the likelihood of observing a shell with a particular postmortem age in the mixed layer, not the likelihood of observing a shell whose age is the actual time of its loss from the assemblage, a critical distinction. To evaluate the fit of density functions to AFDs, we (1) use the Akaike information criterion that penalizes log-likelihood by the number of parameters (Burnham and Anderson, 2002) and (2) compare the observed and modeled estimates of median age and total age range. We use three density functions to estimate unbiased loss rates from AFDs (Fig. 1).

One-Phase Exponential Density (Constant Loss Rate)

In the one-phase model, every shell experiences the same instantaneous probability λ of disappearing, regardless of its postmortem age and its position within the mixed layer, until it is buried to deeper zones where loss becomes ~0 (final burial zone; maturation zone of Sadler, 1993). The loss rate λ thus subsumes both disintegration in the mixed layer and burial below the mixed layer.

Weibull Density (Gradual Decline in Loss Rate)

In the Weibull model, the loss rate is determined by two parameters, *r* and *k*, where *r* is a baseline rate in the exponential function (Gelman et al., 2004). The loss rate experienced by a shell declines over time if the exponent $k < 1$. The decrease in rate (1) might reflect gradual burial if shells experience less severe conditions with greater depth below the sediment-water interface, and/or (2) can occur if diagenetic processes gradually stabilize shells, with or without burial. All burial steps are incrementally slow.

Two-Phase Exponential Density (Abrupt Decline in Loss Rate)

In the two-phase model, an initial, relatively high disintegration rate λ_1 in the TAZ is replaced abruptly by a slower disintegration rate λ_2 in the SZ at a sequestration rate τ that describes the net movement of shells from high to low rates. τ is independent of loss rates. Shells can be shifted to the lower loss rate via a sudden large-increment burial event or by crossing a diagenetic threshold to lower reactivity, with or without burial. This model builds upon a two-phase model where two exponential distributions are separated by a fixed time *T* (Foote, 2001; Krug et al., 2009), but we permit the shift to occur at a random time, following an exponential distribution with rate τ. The right-censored probability density is

$$g(t) = (1-\beta)(\tau+\lambda_1)e^{-(\tau+\lambda_1)t} + \beta\lambda_2 e^{-\lambda_2 t}, \qquad (1)$$

where $\beta = \tau(\tau + \lambda_1) / [\tau(\tau + \lambda_1) + (\lambda_1 - \lambda_2)\,\lambda_2]$. Although exhumation of shells or other reactivation of high loss rates is not accounted for directly, τ can be interpreted as a net sequestration rate under such conditions.

RESULTS

The AFDs of both species are right-skewed, with long tails containing shells as old as ca. 2550 yr to ca. 11,900 yr (Fig. 2). Six of the eight AFDs are qualitatively L-shaped, dominated by shells <100 yr old. Median shell ages in five of them are <50 yr. If loss rates were constant, the age range of an AFD could be predicted by median age alone for a given sample size (black diagonal lines in Fig. 3A). Instead, six of eight assemblages (open symbols in Fig. 3A) fall significantly above this line, with age ranges approximately two orders of magnitude larger than their median ages, much larger than would be generated by a one-phase process. Of the two AFDs close to this line (both *N. taphria*), the Palos Verdes assemblage lacks the mode of young shells at 50 yr, and the San Pedro assemblage has an especially large proportion of old shells, with a secondary mode at 5 k.y. (Fig. 2).

Only Weibull and two-phase models can sufficiently decouple age range from median age to generate the large skewness (>2) observed in most Southern California shell assemblages

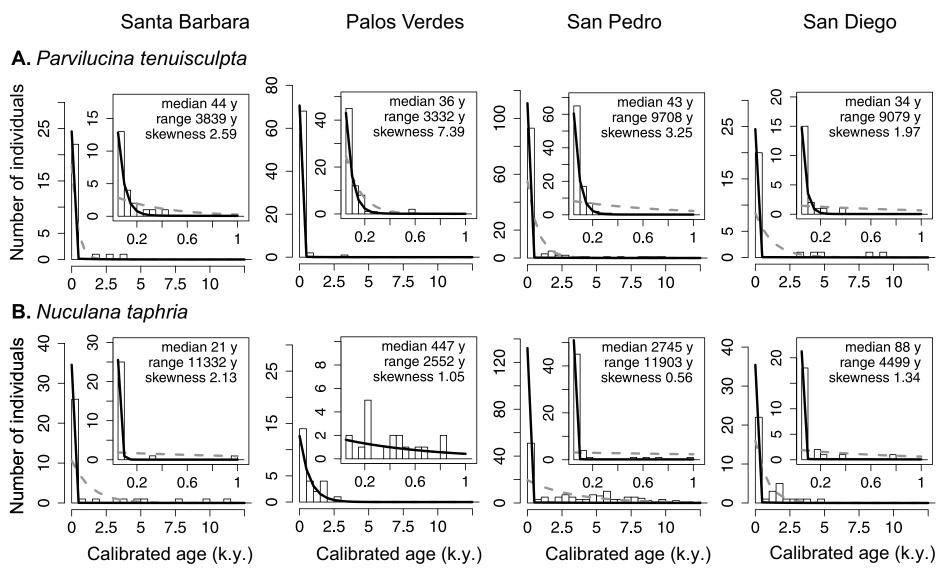

Figure 2. Postmortem age-frequency distributions (AFDs) of shells of *Parvilucina tenuisculpta* (A) and *Nuculana taphria* (B) from four regions within Southern California Bight (USA), calibrated in years before A.D. 2003. Inset plots display AFDs of shells from the most recent 1000 yr. Curves show the fit of a one-phase model in which disintegration rates are constant (dashed gray line; Fig. 1A), which is the current paradigm used to quantify shell loss dynamics, and the fit of our two-phase model with an abrupt decrease in disintegration rates (solid black line; Fig. 1C).

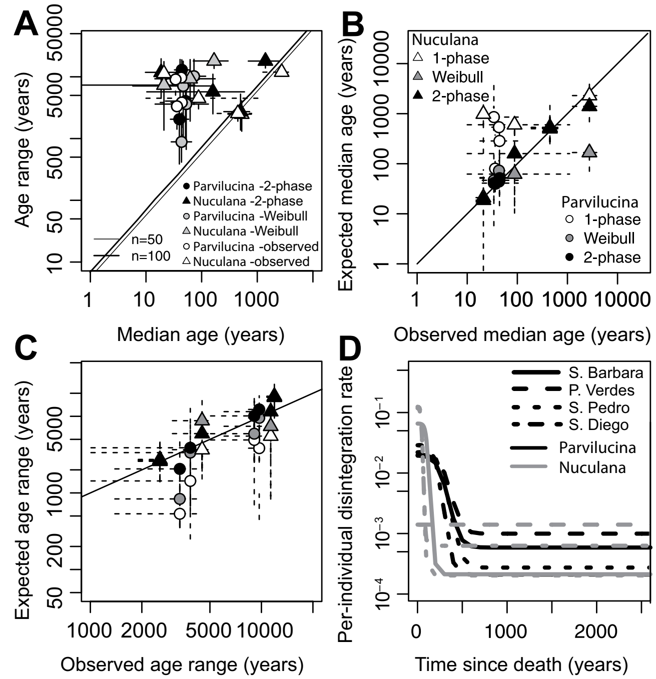

Figure 3. Comparison of observed data with model predictions. A: Black diagonal lines represent the expected relationship between median age and age range when disintegration rates are constant over time (n = 50 and 100 individuals). In the Weibull and two-phase models, median age and age range are strongly decoupled (fall above diagonal lines). Of eight assemblages (white symbols), six have age-frequency distributions (AFDs) that fall above the diagonals; their values are more closely predicted by a two-phase model where disintegration rate decreases abruptly within the mixed layer (black symbols) than by a Weibull model (gray symbols). Error bars represent 95% bootstrapped confidence intervals. B, C: Comparing expected and observed medians (B) and ranges (C) of shell ages, a two-phase model predicts observed values better than a one-phase model in seven of eight assemblages (some symbols hidden; symbols in C are the same as those in B). D: Two-phase model estimates that, with one exception, average per-individual disintegration rates decrease by more than two orders of magnitude within the first few centuries postmortem. S. Barbara—Santa Barbara; P. Verdes—Palos Verdes; S. Pedro—San Pedro; S. Diego—San Diego.

(Fig. 2). Akaike weights show that seven AFDs are better explained by time-varying models than by a one-phase model, and six of these are better explained by our two-phase model with an abrupt decline in disintegration rate (Akaike weights equal to 1; Table DR4). The Weibull model that accurately decouples median age and age range in one case has a very low k (0.19), implying an almost step-like decline in disintegration. Only the two-phase model results in a strong correlation between expected and observed median ages (Pearson r = 0.946; Fig. 3B) and between expected and observed total age ranges (r = 0.94; Fig. 3C). L-shaped AFDs are not artifacts of pooling local AFDs having different shapes. Even at the site level, Akaike weights support time-varying models: seven of 17 local assemblages conform to our two-phase model, and eight conform to the Weibull model (Table DR5).

DISCUSSION

All three models assume that shells enter a death assemblage at a constant rate. Constant production over hundreds to thousands of years is unlikely, but the precise effects on model fitting of violating this assumption are poorly known. The effect should be strongest when changes in production have occurred within the last few high-loss half-lives, i.e., here, within the past few decades. Variability in the deep past will have less effect on model fitting because older cohorts are increasingly rare. Our samples come from water depths with living populations of our two species between A.D. 1990 and 2008, ensuring that death assemblages were receiving fresh shells over the past two decades (Figs. DR6 and DR7). Population densities of both species have been very small (<6 individuals per 0.1 m^2; Table DR1), without any recent increase that could be solely responsible for the initial steep slope of the AFDs (*Parvilucina* populations were high in the 1970s on the Palos Verdes shelf but declined strongly in the mid-1980s; see the Data Repository).

The only exception is *N. taphria* on the Palos Verdes shelf, where it is rare in living assemblages compared to its living abundance in other regions and compared to its abundance in Palos Verdes death assemblages, implying a decline in the supply of young shells. This Palos Verdes AFD is better fit by the one-phase model, with a λ_1 one order of magnitude lower than the λ_1 in other regions. Where λ_1 is high, a recent drop in shell production will inevitably reduce the initial slope of an AFD because the young shells needed to accurately determine λ_1 will be rare. The gentle initial slope of this AFD thus largely reflects disintegration rates in the SZ rather than in the TAZ. This flattening of the initial slope implies that AFDs will be less skewed and even normal both (1) in regions with reduced or inactive production, and (2) with depth down-core, where assemblages are no longer refreshed by newly dead shells, unless (3) sudden burial sequesters the entire mixed layer from the TAZ (see Kidwell, 2013). L-shaped AFDs receiving new shells are thus not a random subset of AFD shapes (e.g., Scarponi et al., 2013), but should be suitable for obtaining unbiased estimates of disintegration and sequestration, and, moreover, commonly characterize published mixed-layer assemblages (Kidwell, 2013).

Based on their AFDs, individual shells in Southern California shift from having decadal half-lives to millennial half-lives: shells completely disintegrate unless they are sequestered within the first few hundred years postmortem (Fig. 3D). The median time to sequestration—e.g., for burial to deeper parts of a mixed layer or for development of diagenetic microenvironments—is very long, ranging between ~1300 and 7500 yr for *Nuculana* and between ~1600 and 8200 yr for *Parvilucina* (Table DR4). Such low sequestration rates suggest lower rates of siliciclastic accretion than documented on the pre–20th century Southern California shelf (~0.1 cm/yr over a 100 yr scale; Alexander and Lee, 2009) and, combined with high initial rates of disintegration, should act against the preservation of very old shells. Assuming steady-state production over the course of time-averaging, our two-phase model estimates that in fact only 0.2%–0.7% of all shell input on this shelf is preserved. This is consistent with observations that the carbonate content of the Southern California seabed is extremely low compared to the expected productivity of the shelly benthos (Smith, 1971) and that diagenetic precipitation is slow in temperate latitudes (Nelson and James, 2000). A range of loss rates is possible on tropical shelves (Best et al., 2007).

The old shells encountered in the mixed layer are from species with low durability. They are aragonitic, small-bodied (2–11 mm), and either thin shelled (*Parvilucina*) or dominated by microbially vulnerable high-organic microstructures (*Nuculana*); preferential preservation of larger shells does not produce the L-shape of the AFDs (Fig. DR8). Long-term survival of carbonate particles in the mixed layer is thus not limited to stereotypic robust oysters and coral heads. The 10–15-cm-thick, decadal-scale mixed layer (Alexander and Lee, 2009) and high abundance of burrowers (Stull et al., 1996) on the Southern California shelf suggest a high probability of vertical mixing of shells, which could blur TAZ and SZ layers. Therefore, some permanent diagenetic stabilization of shells, for example by Ostwald ripening (Aller, 2014), may be necessary to ensure that shells do not revert to λ_1 if moved back to the TAZ.

CONCLUSIONS

Using AFDs that are relatively straightforward to acquire, we provide the first analytical resolution of time-varying disintegration rates in carbonate particles, and demonstrate the critical role of sequestration in permitting their long-term persistence in the mixed layer. Our two-phase model accounts more completely for empirical data than do conceptual models of a single half-life or gradual decline in loss rates with burial, and moreover makes AFDs readable in mechanistic terms. It disentangles and quantifies the key rates of disintegration (slopes) and time to sequestration (burial or stabilization; influences kink in the L-shape) that govern shell loss and persistence, suggesting, for example, a way to measure the effects of ocean acidification. The model allows disintegration rates to be reset diagenetically with or without burial, a phenomenon that can promote long-term persistence under conditions of low net sedimentation. The new model thus both explains the dynamics of carbonate accumulation in modern seabeds in rigorous and realistic terms, and provides a heuristic framework for studying large-scale controls on the completeness and time-averaging of fossil assemblages.

ACKNOWLEDGMENTS

We thank A. Ranasinghe for arranging release of death assemblages from the Bight'03 survey; R. Velarde, D. Cadien, and T. Parker for insights into regional benthos; D. Jablonski, K. Voorhies, K. Rittenbush, E. Edinger, and three anonymous persons for helpful reviews; and funding from the University of Southern California Sea Grant Program (NOAA), the U.S. National Science Foundation (grants EAR-0345897, EAR-1124189, and EAR-1234413), the Slovak Research and Development Agency (APVV 0644-10), and the Scientific Slovak Grant Agency (VEGA 0068-11).

REFERENCES CITED

Alexander, C.R., and Lee, H.J., 2009, Sediment accumulation on the Southern California Bight continental margin during the twentieth century, *in* Lee, H.J., and Normark, W.R., eds., Earth Science in the Urban Ocean: The Southern California Continental Borderland: Geological Society of America Special Paper 454, p. 69–87, doi:10.1130/2009.2454(2.4).

Aller, R.C., 1982, Carbonate dissolution in nearshore terrigenous muds: The role of physical and biological reworking: The Journal of Geology, v. 90, p. 79–95, doi:10.1086/628652.

Aller, R.C., 2014, Sedimentary diagenesis, depositional environments, and benthic fluxes, *in* Holland, H.D., and Turekian, K.K., eds.,Treatise on Geochemistry, Volume 8: The Oceans and Marine Geochemistry: Oxford, Elsevier, p. 293–334.

Best, M.M.R., Ku, T.C., Kidwell, S.M., and Walter, L.M., 2007, Carbonate preservation in shallow marine environments: Unexpected role of tropical siliciclastics: The Journal of Geology, v. 115, p. 437–456, doi:10.1086/518051.

Burnham, K.P., and Anderson, D.R., 2002, Model Selection and Multimodel Inference: A Practical Information-Theoretic Approach (second edition): New York, Springer, 488 p.

Cummins, H., Powell, E.N., Stanton, R.J., Jr., and Staff, G., 1986, The rate of taphonomic loss in modern benthic habitats: How much of the potentially preservable community is preserved?: Palaeogeography, Palaeoclimatology, Palaeoecology, v. 52, p. 291–320, doi:10.1016/0031-0182(86)90052-0.

Davies, D.J., Powell, E.N., and Stanton, R.J., 1989, Relative rates of shell dissolution and net sediment accumulation: A commentary: Can shell beds form by the gradual accumulation of biogenic debris on the seafloor?: Lethaia, v. 22, p. 207–212, doi:10.1111/j.1502-3931.1989.tb01683.x.

Edinger, E.N., Burr, G.S., Pandolfi, J.M., and Ortiz, J.C., 2007, Age accuracy and resolution of Quaternary corals used as proxies for sea level: Earth and Planetary Science Letters, v. 253, p. 37–49, doi:10.1016/j.epsl.2006.10.014.

Emery, K.O., 1968, Relict sediments on continental shelves of the world: The American Association of Petroleum Geologists Bulletin, v. 52, p. 445–464.

Flessa, K.W., and Kowalewski, M., 1994, Shell survival and time-averaging in nearshore and shelf environments: Estimates from the radiocarbon literature: Lethaia, v. 27, p. 153–165, doi:10.1111/j.1502-3931.1994.tb01570.x.

Foote, M., 2001, Evolutionary rates and the age distributions of living and extinct taxa, *in* Jackson, J.B.C., et al., eds., Evolutionary Patterns: Growth, Form, and Tempo in the Fossil Record: Chicago, University of Chicago Press, p. 245–295.

Gelman, A., Carlin, J.B., Stern, H.S., and Rubin, D.B., 2004, Bayesian Data Analysis (second edition): Boca Raton, Florida, Chapman and Hall, 696 p.

Glover, C.E., and Kidwell, S.M., 1993, Influence of organic matrix on the post-mortem destruction of molluscan shells: The Journal of Geology, v. 101, p. 729–747, doi:10.1086/648271.

Kidwell, S.M., 1986, Models for fossil concentrations: Paleobiologic implications: Paleobiology, v. 2, p. 6–24.

Kidwell, S.M., 2013, Time-averaging and fidelity of modern death assemblages: Building a taphonomic foundation for conservation paleobiology: Palaeontology, v. 56, p. 487–522, doi:10.1111/pala.12042.

Kidwell, S.M., and Bosence, D.W.J., 1991, Taphonomy and time-averaging of marine shelly faunas, *in* Allison, P.A., and Briggs, D.E.G., eds., Taphonomy, Releasing the Data Locked in the Fossil Record: New York, Plenum Press, p. 115–209.

Kidwell, S.M., Best, M.M.R., and Kaufman, D.S., 2005, Taphonomic trade-offs in tropical marine death assemblages: Differential time averaging, shell loss, and probable bias in siliciclastic vs. carbonate facies: Geology, v. 33, p. 729–732, doi:10.1130/G21607.1.

Kosnik, M.A., Hua, Q., Kaufman, D.S., and Wüst, R.A., 2009, Taphonomic bias and time-averaging in tropical molluscan death assemblages: Differential shell half-lives in Great Barrier Reef sediment: Paleobiology, v. 35, p. 565–586, doi:10.1666/0094-8373-35.4.565.

Kosnik, M.A., Kaufman, D.S., and Hua, Q., 2013, Radiocarbon-calibrated multiple amino acid geochronology of Holocene molluscs from Bramble and Rib reefs (Great Barrier Reef): Quaternary Geochronology, v. 16, p. 73–86, doi:10.1016/j.quageo.2012.04.024.

Kowalewski, M., Goodfriend, G.A., and Flessa, K.W., 1998, High-resolution estimates of temporal mixing within shell beds: The evils and virtues of time-averaging: Paleobiology, v. 24, p. 287–304.

Krause, R.A., Barbour, S.L., Kowalewski, M., Kaufman, D.S., Romanek, C.S., Simoes, M.G., and Wehmiller, J.F., 2010, Quantitative comparisons and models of time-averaging in bivalve and brachiopod shell accumulations: Paleobiology, v. 36, p. 428–452, doi:10.1666/08072.1.

Krug, A.Z., Jablonski, D., and Valentine, J.W., 2009, Signature of the end-Cretaceous mass extinction in the modern biota: Science, v. 323, p. 767–771, doi:10.1126/science.1164905.

Meldahl, K.H., Flessa, K.W., and Cutler, A.H., 1997, Time-averaging and postmortem skeletal survival in benthic fossil assemblages: Quantitative comparisons among Holocene environments: Paleobiology, v. 23, p. 207–229.

Morse, J.W., and Casey, W.H., 1988, Ostwald processes and mineral paragenesis in sediments: American Journal of Science, v. 288, p. 537–560, doi:10.2475/ajs.288.6.537.

Nelson, C.S., and James, N., 2000, Marine cements in mid-Tertiary cool-water shelf limestones of New Zealand and southern Australia: Sedimentology, v. 47, p. 609–629, doi:10.1046/j.1365-3091.2000.00314.x.

Olszewski, T., 1999, Taking advantage of time-averaging: Paleobiology, v. 25, p. 226–238.

Olszewski, T.D., 2004, Modeling the influence of taphonomic destruction, reworking, and burial on time-averaging in fossil accumulations: Palaios, v. 19, p. 39–50, doi:10.1669/0883-1351(2004)019<0039:MTIOTD>2.0.CO;2.

Powell, E.N., Kraeuter, J.N., and Ashton-Alcox, K.A., 2006, How long does oyster shell last on an oyster reef?: Estuarine, Coastal and Shelf Science, v. 69, p. 531–542, doi:10.1016/j.ecss.2006.05.014.

Powell, E.N., Staff, G.M., Callender, W.R., Ashton-Alcox, K.A., Brett, C.E., Parsons-Hubbard, K.M., Walker, S.E., and Raymond, A., 2011, Taphonomic degradation of molluscan remains during thirteen years on the continental shelf and slope of the northwestern Gulf of Mexico: Palaeogeography, Palaeoclimatology, Palaeoecology, v. 312, p. 209–232, doi:10.1016/j.palaeo.2010.12.006.

Sadler, P.M., 1993, Models of time-averaging as a maturation process: How soon do sedimentary sections escape reworking?, *in* Kidwell, S.M., and Behrensmeyer, A.K., eds., Taphonomic Approaches to Time Resolution in Fossil Assemblages: Paleontological Society Short Courses in Paleontology 6, p. 188–209.

Scarponi, D., Kaufman, D., Amorosi, A., and Kowalewski, M., 2013, Sequence stratigraphy and the resolution of the fossil record: Geology, v. 41, p. 239–242, doi:10.1130/G33849.1.

Smith, S.V., 1971, Budget of calcium carbonate, Southern California continental borderland: Journal of Sedimentary Petrology, v. 41, p. 798–808.

Stuiver, M., and Reimer, P.J., 1993, Extended ^{14}C database and revised CALIB radiocarbon calibration program: Radiocarbon, v. 35, p. 215–230.

Stull, J.K., Swift, D.J.P., and Niedoroda, A.W., 1996, Contaminant dispersal on the Palos Verdes continental margin: I. Sediments and biota near a major California wastewater discharge: The Science of the Total Environment, v. 179, p. 73–90, doi:10.1016/S0048-9697(96)90050-9.

Waldbusser, G.G., Steenson, R.A., and Green, M.A., 2011, Oyster shell dissolution rates in estuarine waters: Effects of pH and shell legacy: Journal of Shellfish Research, v. 30, p. 659–669, doi:10.2983/035.030.0308.

Manuscript received 20 March 2014
Revised manuscript received 24 June 2014
Manuscript accepted 25 June 2014

Printed in USA